

Physical modelling of laboratory debris flows by using the Sodium Carboxymethylcellulose (Na-CMC)

GIACOMO VICCIONE, MARCO GENOVESE, FABIO ROSSI

Department of Civil Engineering (DICIV)

University of Salerno

Via Giovanni Paolo II n. 132, 84084 Fisciano

ITALY

mgenovese@unisa.it, gviccion@unisa.it, f.rossi@unisa.it <http://www.diciv.unisa.it/docenti>

DOMENICO GUIDA, TONY LUIGI LEOPOLDO LENZA

Department of Industrial Engineering (DIIN)

University of Salerno

Via Giovanni Paolo II n. 132, 84084 Fisciano

ITALY

guida@unisa.it, lenza@unisa.it <http://www.diin.unisa.it/struttura/docenti>

Abstract: Debris flows are among the most destructive processes occurring in mountain environments. It is recognized that rheology describing the relationship between stress and strain rates is mainly dependent from interstitial fluid content, pore fluid pressure, sediment concentration, and size and distribution of dispersed grains. However, due to their complex behaviour, it is unlikely that they can be characterized by a prefixed rheological model. Within this framework, we have assessed the feasibility of a double model of similarity of Reynolds and Froude, as attempt to mimicking the interstitial fluid phase at laboratory scale. For the purpose we used the Sodium Carboxymethylcellulose (Na-CMC or briefly CMC) as thickening agent in aqueous solutions. By varying the solute concentration, it was possible to reproduce the pore fluid of a specific viscosity.

The related transparency of such solutions allows observing and describing evolution processes by high-frequency digital acquisition. Among the others, the main innovative feature consisted in the possibility of establishing a relationship between laboratory experiments and corresponding assumed prototypes, by means of the proposed model scaling.

The experimental campaign being carried out, allowed to establish a state equation for the model reference, that is a relationship among viscosity, solute concentration and temperature. A predominant dependence between viscosity and solute concentration was observed, marking another advantage in using such solutions. The similarity then connect model results to the prototype.

Key-Words: - **Debris flows – Interstitial fluid – Sodium Carboxymethylcellulose – Na-CMC – Physical modelling – model scaling – Viscosity – viscometric tests – Rheological models.**

1 Introduction

In the last few decades, debris flows [1-3] have been extensively studied by the scientific community involved in, because of their potentially destructive power associated. Numerical investigations of triggering, propagation, amplification and deposition processes aimed at the definition of advanced models, see e.g. [4-7]. Still, they are based on simplifying assumptions.

For instance, the related hazard assessment relies on empirical or semi-empirical hydraulic resistance formulae; the shear stress between channel boundaries and the flowing mass is currently

determined by relationships, developed in non-hydrodynamic contests, e.g. the Coulomb law describing the shear stress τ as function of the cohesion c , the normal stress σ and the friction angle ϕ .

As matter of facts, rheological laws need to be first validated via experimental investigation [8-11], depending on the particular phenomenon observed.

As commonly known, laboratory investigation relies on scale models. More precisely, once ruling parameters are identified, scaling models are established, in which the weight of such variables is assumed to be relevant. The lower is the number of

variables omitted, the greater is the accuracy in reproducing the real phenomenon at laboratory scale.

In this framework, starting from references [12,13], this work further investigates about the feasibility of a double model of similarity of Reynolds and Froude, as attempt to mimicking the interstitial fluid phase in debris flows kind of phenomena. For the purpose, water solutions of Sodium Carboxymethylcellulose (Na-CMC or strictly CMC) are used for the fluid in the model.

Also known as cellulose gum, the CMC is an anionic water-soluble polymer derived from the cellulose. It is widely used as an economical viscosity modifier or thickener in different sectors of industry and technology. Applications can be found in pharmaceutical or fabric manufacturing, in orthopedic surgery as lubricant for articulations, in wine industry, in foods and beverages for its stabilizing effects or even for the production of cigarettes. An example in Civil Engineering is related to its use as alternative to drilling mud during well perforation.

Despite the existence in literature of studies concerning the use of chemical additives as rheological modifiers (e.g. see [14]), to the authors knowledge there are no specific experimental investigations related to the use of CMC-water solutions as attempt to mimicking the interstitial fluid in laboratory debris flows. As matter of facts, there are relevant advantages in such cases. In particular, accurate viscosity values can be attained as function of the employed CMC concentration; the rheological behaviour of the CMC-water solutions is slightly pseudo-plastic, hence approximable to the Newtonian relationship for low rates of deformation; the related transparency of such solutions allows observing and describing evolution processes on flumes boundaries by high-frequency digital camera acquisition. A special experimental apparatus, designed by the Authors, has been then designed (see Figure 1).

2 The model of similitude

Advantages, previous mentioned, suggest the use of the CMC as viscosity modifier for modelling the interstitial fluid in laboratory debris flows.

The similitude model, next proposed, takes into account the scale effect between the laboratory experiment (model) and the corresponding real event (reference prototype).

Viscosity values to be imposed for the model are then derived.

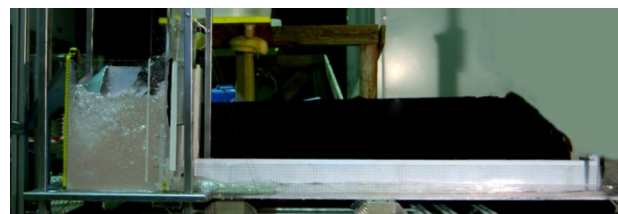


Fig. 1. CMC-water solutions can be conveniently used in open channel flow laboratory investigations.

Commonly known, physical modelling of real events is based on the equality, between model and prototype, of specific dimensionless quantities, that is of specific index numbers. It is worth recalling that such groupings are determined as function of those physical quantities judged to be relevant for a comprehensive description of the phenomenon at hand. By recalling the Buckingham theorem, if a physical phenomenon is described by n variables, r of which independent, then $n-r$ dimensionless grouping numbers can be established for its comprehensive description. Therefore, it is possible to migrate from a relationship, usually unknown, which bonds n variables $(\alpha, \beta, \gamma, \dots, \delta_n)$, to a new one, describing the dependence among $n-r$ dimensionless parameters, that is:

$$f(\alpha, \beta, \gamma, \dots, \delta_n) = 0 \Rightarrow F(\pi_1, \pi_2, \pi_3, \dots, \pi_{n-r}) = 0 \quad (1)$$

being π_i the so called index numbers of the physical modelling. In principle, they should be the same in the model and the prototype – yielding a full model of similarity – a condition that cannot be achieved in practice.

The aim here is to derive viscosity values of CMC-water solutions to be used in laboratory investigation for the analysis of debris flows kind of phenomena. They are characterized by a particular type of motion, known as “granular”, which can be assumed half way between quasi-static regimes, typical of landslides, and hydrodynamic regimes, typical of dilute suspensions [15]. Granular regimes can be at low, intermediate or high velocity of deformation. The motion is said to be: in the first case “macro-viscous”, in the intermediate case “of transition” while in the latter case is said to be “inertial”. The regime of motion can be identified by two dimensionless parameters [16]. The dispersed Reynolds number

$$R_d = \left(\frac{T_{xy}}{c_1} \rho_s \right)^{1/2} \frac{d_s}{\mu} \quad (2)$$

and the Bagnold number

$$B = \frac{c_1^{1/2}}{\mu} \rho_s d_s^2 \frac{du}{dy} \quad (3)$$

where T_{xy} is the dispersed shear stress, ρ_s and d_s are the density and the reference size of the solid phase, μ the dynamic viscosity, c_1 the linear concentration and du/dy the velocity of deformation.

Other approaches, developed more recently, are available for identifying the working regime, see for instance [17].

$R_d > 55$ and $B > 450$ correspond to the inertial kind of regime. In this case the contribution of gravitational terms is predominant. The phenomenon can be described by a Froude model of similarity.

$R_d < 10$ and $B < 40$ matches the case of the macro-viscous regime. Viscous stresses are predominant respect the inertial ones. Tangential and normal stresses are linear function of the velocity of deformation. In this case, the phenomenon can be described by a Reynolds model of similarity.

Debris flows are half way the cases aforementioned [18], therefore it is necessary (see for instance [19] and the appendix of [18]) taking into account the contribution of both viscous and gravitational terms. This can be done by coupling Reynolds and Froude models of similarity. The double similitude is achievable by only imposing a specific relationship between model and prototype viscosities. In facts, assuming the following parameters: viscosity μ , density ρ , velocity V , spatial scale l and referring them to the prototype and the model with subscript p and m respectively, the equality of Reynolds numbers can be rewritten as:

$$\frac{\rho_m l_m V_m \mu_p}{\rho_p l_p V_p \mu_m} = 1 \quad (4)$$

yielding

$$\frac{V_m}{V_p} = \frac{\mu_m l_p}{\mu_p l_m} \quad (5)$$

in the case of same densities, a condition fulfilled as long as low molecular weight of CMC is used [20]. The equality of Froude numbers yields:

$$\frac{V_m \sqrt{g_p \cdot l_p}}{V_p \sqrt{g_m \cdot l_m}} = 1 \quad (6)$$

or more concisely:

$$\frac{V_m}{V_p} = \frac{\sqrt{l_m}}{\sqrt{l_p}} \quad (7)$$

as the acceleration of gravity is expected to be the same in the model and the prototype.

By combining eqs (5) and (7) the next equation is given

$$\mu_m = \mu_p \left(\frac{l_m}{l_p} \right)^{3/2} = \mu_p \cdot \lambda^{3/2} \quad (8)$$

where λ is the assumed spatial scale between model and prototype. Eq. (8) sets a relationship between viscosities in the model “m” and prototype “p”. Assuming a specific interstitial fluid in the prototype, i.e. μ_p , eq. (8) implies that the double Reynolds-Froude similitude model can be established only adopting for the model a solution of a certain viscosity. Such a condition is not always achievable. In facts, since the prototype is commonly scaled down, follows that $0 < \lambda < 1$.

As typical viscosity μ_p values of the inner fluid in real debris flows range from water’s ($\mu_w = 1 \times 10^{-3}$ Pa*s) to 10^2 Pa*s (intended as maximum order of magnitude), it is possible to reproduce the prototype only if $\mu_m \geq \mu_w$. As for instance, considering a fluid featuring the same viscosity μ_w of water, a geometric length scale $\lambda=0.1$ would imply the use of a fluid with a viscosity value being equal to 3.16×10^{-5} Pa*s for the model, which is not consistent. Such a limitation is not so tightening as real interstitial fluids are commonly made up of water and fine sediments, hence with an associated viscosity greater (or much greater) than water’s.

Fixing λ , it is always possible to determine a lower limit of viscosity μ_p above which the corresponding fluid can be scaled, that is $\mu_m > \mu_w$. The closer is λ to the unity, the greater is the range of reproducibility: for the limit value $\lambda=1$, eq. (8) yields $\mu_m=\mu_p$, i.e. model and prototype are the same. Let us consider the simplified case of mudflows analyzed by O’Brien and Julien [21], made up of 30% of clay. Solid concentration c_v , ranging from 0 to 0.6 is related to the dynamic viscosity μ_p as next shown in Table 1 and 2. As can be seen, fixing $\lambda=0.05$ (see Table 1) allows reproducing mudflows with solid concentration $c_v > 0.13$ (bold marked).

Increasing λ allows reproducing a greater range of solid concentrations. In facts, for $\lambda=0.1$ the lower limit is $c_v>0.03$ (see Table 2).

c_v [-]	μ_p [Pa*s]	μ_m [Pa*s]	Check
0.60	311.77	3.49E+00	√
0.58	196.81	2.20E+00	√
0.56	124.25	1.39E+00	√
0.54	78.44	8.77E-01	√
0.52	49.52	5.54E-01	√
0.50	31.26	3.49E-01	√
0.48	19.73	2.21E-01	√
0.46	12.46	1.39E-01	√
0.44	7.87	8.79E-02	√
0.42	4.97	5.55E-02	√
0.40	3.14	3.51E-02	√
0.38	1.98	2.21E-02	√
0.36	1.25	1.40E-02	√
0.34	0.79	8.84E-03	√
0.32	0.50	5.58E-03	√
0.30	0.32	3.53E-03	√
0.28	0.20	2.24E-03	√
0.26	0.13	1.42E-03	√
0.24	0.08	9.02E-04	NO
0.22	0.05	5.75E-04	NO
0.20	0.03	3.69E-04	NO
0.18	0.02	2.39E-04	NO
0.16	0.01	1.56E-04	NO
0.14	0.01	1.04E-04	NO
0.12	0.01	7.05E-05	NO
0.10	0.00	4.93E-05	NO
0.00	0.00	1.47E-05	NO

Table 1. Viscosity μ_p values of mudflows analyzed in [21] and corresponding μ_p for $\lambda=0.05$. Red values are not reproducible in principle, since $\mu_m<\mu_w$ (clear water).

The model of similitude being established, requires not only that the measured viscosity can be transferred to the prototype and vice-versa (see eq. 8). Scaling factors must be in a certain relationship. To clarify this issue, let us introduce the geometric scale λ , the mass scale m and the time scale τ as follows:

$$\lambda = \frac{l_m}{l_p} \quad m = \frac{m_m}{m_p} \quad \tau = \frac{t_m}{t_p} \quad (9)$$

Keeping the same liquid (i.e. $\rho_p = \rho_m$ or $\frac{\rho_p}{\rho_m} = 1$)

implies that $\frac{m}{\lambda^3} = 1$, that is

$$m = \lambda^3 \quad (10)$$

On the other and, since gravity is constant (i.e. $g_p = g_m$) follows that $\frac{\lambda}{\tau^2} = 1$ or

c_v [-]	μ_p [Pa*s]	μ_m [Pa*s]	Check
0.60	311.77	9.86E+00	√
0.58	196.81	6.22E+00	√
0.56	124.25	3.93E+00	√
0.54	78.44	2.48E+00	√
0.52	49.52	1.57E+00	√
0.50	31.26	9.89E-01	√
0.48	19.73	6.24E-01	√
0.46	12.46	3.94E-01	√
0.44	7.87	2.49E-01	√
0.42	4.97	1.57E-01	√
0.40	3.14	9.92E-02	√
0.38	1.98	6.26E-02	√
0.36	1.25	3.96E-02	√
0.34	0.79	2.50E-02	√
0.32	0.50	1.58E-02	√
0.30	0.32	9.99E-03	√
0.28	0.20	6.33E-03	√
0.26	0.13	4.01E-03	√
0.24	0.08	2.55E-03	√
0.22	0.05	1.63E-03	√
0.20	0.03	1.04E-03	√
0.18	0.02	6.75E-04	NO
0.16	0.01	4.41E-04	NO
0.14	0.01	2.93E-04	NO
0.12	0.01	1.99E-04	NO
0.10	0.00	1.39E-04	NO
0.00	0.00	4.16E-05	NO

Table 2. Viscosity μ_p values of mudflows analyzed in [21] and corresponding μ_p for $\lambda=0.1$. In this case, a wider range of concentrations can be modeled (i.e. for $c_v>0.03$).

$$\lambda = \tau^2 \quad (11)$$

Lastly, since eq. (8) can be rewritten as $\frac{\mu_p}{\mu_m} = \lambda^{3/2}$

follows that $\frac{m}{\lambda \cdot \tau} = \lambda^{3/2}$ or simplifying

$$\frac{m}{\tau} = \lambda^{5/2} \quad (12)$$

It is simple to ascertain that combining two of the above eqs. (10) - (12) yields back the remaining one. All physical dimensionless quantities can be therefore expressed as function of one of the scales introduced in eqs. (9). As for instance, the velocity ratio turns out to be

$$\frac{V_m}{V_p} = \frac{\lambda}{\tau} = \frac{\lambda}{\lambda^{1/2}} = \lambda^{1/2} \quad (13)$$

for discharges:

$$\frac{Q_m}{Q_p} = \frac{\lambda^3}{\tau} = \frac{\lambda^3}{\lambda^{1/2}} = \lambda^{5/2} \quad (14)$$

for forces:

$$\frac{F_m}{F_p} = \frac{\mu \cdot \lambda}{\tau^2} = \frac{\lambda^3 \cdot \lambda}{\lambda} = \lambda^3 \quad (15)$$

and so on.

3 CMC-water solutions properties

In this section, properties of CMC-water solutions are recalled.

3.1 Viscosity definition

Viscosity plays a key role in numerical modelling of debris flow propagation [22], both in single-equivalent phase [23]-[25] and multi-phase [4], [17], [26,27] continuum approaches. While mass flow is treated as a homogeneous fluid in the former case, obeying a rheologic formulation such as the Bingham or the more generalized Herschel-Bulkley representation, a specific stress-strain relationship for the interstitial fluid has to be imposed in the latter one, being treated separately.

The viscosity of the fluid entrapped in the voids is greater than water's as it is composed by water and fine sediments (e.g. silt, clay, thin sand). Such a solid component of variable concentration, remains suspended inside the interstitial fluid – acting as carrier – thank to the exerted viscous forces. Particles of greater dimensions (>500µm for simplicity), forming the solid component of the whole flowing mass, move downstream while interacting among them [17]. As one can perceive, the physics behind the phenomenon is quite complicated. Huge literature (a small amount is reported in the References) has been produced so far, in attempt to assessing it.

The presence of fine sediments in the interstitial fluid affect both its density ρ_f and dynamic viscosity μ .

Fluid density ρ_f can be evaluated by considering the following weighted averaging:

$$\rho_f = \rho_{\text{fines}} c_{\text{fines}} + \rho_w (1 - c_{\text{fines}}) \quad (16)$$

where ρ_w is the water density while ρ_{fines} and c_{fines} are the density and the concentration of fine sediments respectively. The presence of air is neglected.

For the viscosity parameter μ , there is not an univocal formulation in literature, see for instance [28,29]. It certainly depends on the sediment concentration c_{fines} as well as on the amount of cohesive material, forming the interstitial fluid [30], but it is also function of the local rate of deformation, size distribution and mineralogical properties of fine sediments.

Empirical analysis of O'Brien and Julien [21] allowed to define a general relationship for the dynamic viscosity, as function of c_{fines} , as follows:

$$\mu = \alpha_1 \cdot e^{\beta_1 \cdot c_{\text{fines}}} \quad (17)$$

where the constants α_1 , and β_1 are defined on the basis of the specific experimental case.

CMC-water solution viscosity will depend on the solute concentration and temperature of the mixture as next explained in Section 3.2. On such basis, specific solution concentrations can be reproduced as reference for modelling debris flows at laboratory scale.

3.2 Rheological definition

CMC-water solutions feature a rheological behaviour slightly pseudoplastic, i.e. of shear-thinning type. They can be then approximated as a Newtonian fluid for low rates of deformations [20].

This aspect turns out to be a significant fact towards the aims here pursued. In facts, debris flow movements may be numerically modelled through two distinct mathematical approaches:

- a first one, based on the assumption of the moving of an equivalent fluid: liquid and solid phases are “merged” into a single-phase medium, which is in turn modelled by specific rheological laws, see for instance [31]. Such a simplified interpretation is particularly suitable for wet mass movements in which the coarse granular component is negligible, i.e. in the case of mudflows or hyperconcentrated floods [29];
- a second one, based on the theory of mixtures, in which dynamic stress contributions of solid and liquid phases, generally uncoupled, are separately accounted [17] in the ruling momentum equations. Resulting models are more

complicated to establish than the previous ones, but closer to the reality.

In both approaches, both appropriate viscosity description (of the entire “equivalent moving mass” in the first case, of the interstitial fluid in the second case) and rheology formulation are fundamental.

In single phase continuum models, different stress-strain relationships can be assumed, e.g. based on Bingham, Herschel-Bulkley (as already stated in section 3.1), dilatant fluid of Takahashi [32], or even Newtonian models [33]. In the mixture’s theory, rheology description of the interstitial fluid (water and fine sediments) is related to the concentration of the solid component.

Here, the viscosity field of Na-CMC/water solutions is derived experimentally, assuming a stress-strain relationship based on the Newtonian law, as low rates of deformation are expected. Results are transferred to the real world by means of the similitude model previously described, in order to connect laboratory results with corresponding true viscosities, expected in real events.

Nonetheless, it is worth mentioning that such solutions may exhibit a tixotropic behaviour [20] when undergo to cycles of steady states and stress-strain solicitations. In such cases, the fluid become hysteretic with a time-varying viscosity. To overcome such issue, a single sample of Na-CMC/water solution is recommended to be used once, or more complicated models must be taken into account, to describe the relationship between viscosity and shear rate of deformation, e.g. see [34].

3.3 The transparency feature

Transparency of CMC-water solutions turns out to be useful while carrying laboratory tests in which they are employed. For instance, a propagating viscous mass of solid particles dispersed in a CMC-water solution, acting as interstitial fluid, can be described at the boundaries of a transparent open channel flow laboratory (e.g. see Figure 1), by means of digital images taken with a high speed video camera [35].



Fig. 2. Solute concentration of CMC-water solutions is set by using precision scale and a 250-ml flask.

Kinematics can be therefore described by processing them with a PIV technique. Dynamics can be described as well, by measuring wall stresses [36] by specific sensor probes.

In such a way, the experimentation can provide more meaningful insights than those obtainable from an hypothetic observation of real wet granular flows, in which the interstitial fluid is opaque for the presence of fine components such as silts or clays and, most importantly, banks and channel bed are not transparent, leaving only the free surface to the observer.

4 Materials and methods

4.1 The laboratory equipment

In order to describe the viscosity field of CMC-water solutions as function of solute concentration and temperature, viscosimetric tests were performed at the Department of Industrial Engineering (DIIN), University of Salerno (Italy), employing the digital thermostatic ensemble UTV 190, made by I.S.Co. s.r.l.. It is basically composed by two components: the thermostatic bath and the heater GTR 190. The first one consists of a parallelepiped tank filled by the thermostatic liquid, commonly water. The container can be considered adiabatic. Temperature is kept fixed for the time needed to carry out a single test. The upper cover is composed by an iron plate, four holes provided through which the same number of viscometers can be submerged in the heated liquid.

The heater is composed by a pump and a heating coil through which the moving liquid is heated by an electric resistance. The hydraulic circuit is submerged in the thermostatic bath, together with the temperature probe.

The energy supplied by the electric resistance heats the liquid in the heating coil, which in turn warms up the liquid in the thermostatic bath for convection. Once reached the claimed temperature read at the probe, the bath receives four capillary viscometers,

of Ostwald type. Their diameter is not constant but assumed to be greater for higher concentrations of CMC. This is due to the expected corresponding higher viscosity values.

The preparation of solutions of specific concentrations was performed by means of a precision digital scale (tolerance being 0.1g) and an Erlenmeyer flask (see Fig. 2). The relative procedure for samples attainment is next given.

4.2 Procedure for the preparation of samples

In order to derive the relationship describing the viscosity field as function of solute concentration c and temperature T , 8 different solutions were prepared. The adopted procedure is next given:

1. initial adjustment of the scale (setting to 0) without the sample;
2. weight measurement of an empty and dry flask;
3. re-initialization of the scale (setting to 0) with the empty flask;
4. weight measurement of the flask filled with the desired volume of water;
5. re-initialization of the scale (setting to 0) with an empty and dry flask;
6. weight measurement of the flask filled with the desired CMC content to a desired value;
7. mixing water and solute, knowing their relative weight, that is preparation of a solution with known concentration;
8. cleaning the measurement devices for a new sequence of operations from 1 to 7.

4.3 Experimental tests

After the preparation of samples (see previous section 3.2), a week was then waited for the completion of the related solution processes.

Sample viscosities were then measured by means of the digital thermostatic ensemble UTV 190. For each sample (i.e. for each specific CMC concentration), readings were taken at different temperatures (step approximately set to $\Delta T=5^\circ\text{C}$). The related procedure for measuring the viscosities is next given:

1. filling the four viscometers with as many CMC-water solution samples;
2. introduction of the viscometers into the thermostatic bath through the upper holes;
3. setting temperature of the thermostatic bath to a desired value;
4. keeping the selected temperature for about 15 minutes by means of the heater, in order

to assure that each solution reaches the same temperature level of the bath;

5. test execution was then carried out, following the manufacturer instructions;
6. evaluating the viscosity by means of the following equation:

$$\nu = t \cdot K \quad (4)$$

where ν is the dynamic viscosity in centistokes (cs), t is the test duration in seconds (s), and K is an instrument constant;

7. cleaning and drying of the employed viscometers for a new sequence of operations from 1 to 6.

Test duration t is measured with a digital chronometer (0.1s of precision tolerance).

5. Results

5.1 Relationship between viscosity μ_p , CMC concentration c and temperature T in the prototype.

The functional $\mu_p(c, T)$ is here derived on the basis of the acquired data taken from the experimental investigation described in section 3.3.

Measurements are fitted in order to obtain $\mu_p(c, T)$ as a 3D functional in space. Spatial fitting is performed sequentially, first on the independent variable temperature T and then on the concentration c , having in mind that viscosity increases with the decreasing of the former and increases with the increasing of the latter.

For each sample, the concentration of CMC c is fixed and known. The first regression yields the function:

$$\mu_p = b \cdot m^T \quad (10)$$

with coefficients b and m obtained by applying the generalized least square method.

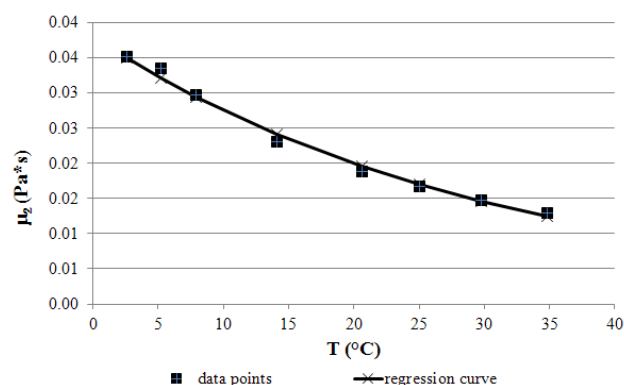


Fig. 3. Regression curve $\mu_p = b \cdot m^T$ for CMC concentration $c = 0.25\%$.

Figure 3 shows the regression curve, obtained for the specific case $c = 0.25\%$. Fittings is quite satisfying as the coefficient of determination is $R_2 = 0.94$. Figure 4 shows the regression applied for all samples, which measured concentration is specified in Table 2. Dependent variable needs to be expressed in logarithmic scale as in this case the model viscosity ranges over four orders of magnitude.

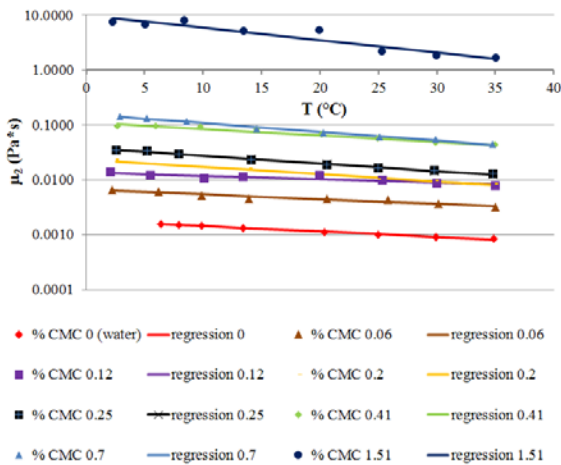


Fig. 4. Regression curves $\mu_p = b \cdot m^T$ for all samples.

c (%)	M	B
0	0.97744	0.00182
0.06	0.98002	0.00670
0.12	0.98539	0.01374
0.2	0.96959	0.02363
0.25	0.96836	0.03803
0.41	0.97326	0.11137
0.7	0.96372	0.15642
1.51	0.94974	9.92663

Table 2. Regression coefficients m and b for all samples prepared.

Coefficients b and m are then regressed on the concentration c , yielding the following power laws:

$$b = \alpha \cdot e^{\beta c} \tag{11}$$

$$m = \chi + \delta \cdot c \tag{12}$$

where coefficients $\alpha, \beta, \chi, \delta$ are next given:

$$\alpha = 0.00829; \beta = 4.693; \chi = 0.9790; \delta = -0.01999.$$

Numerical values of b and m coefficients, as function of concentration of adopted samples, are given by solving eqs. (11) and (12) and reported in Table 2 as well. Substituting the obtained functions $b(c)$ and $m(c)$ (sketched in Figures 5 and 6 respectively) inside the general equation

$$\mu_p(c, T) = b(c) \cdot [m(c)]^T \tag{13}$$

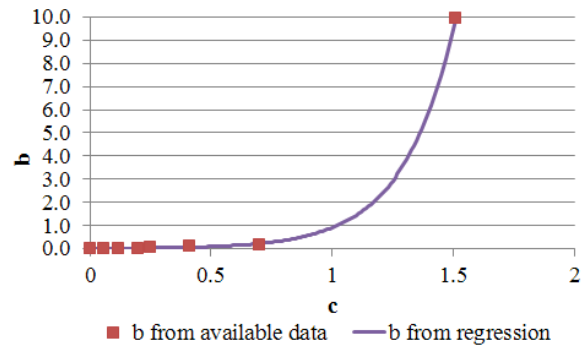


Fig. 5. Regression of the b coefficient on the concentration c . Dots represent available data.

yields the following one:

$$\mu_p(c, T) = 0,008290 \cdot e^{4,693c} \cdot (0,9790 - 0,01999 \cdot c)^T \tag{14}$$

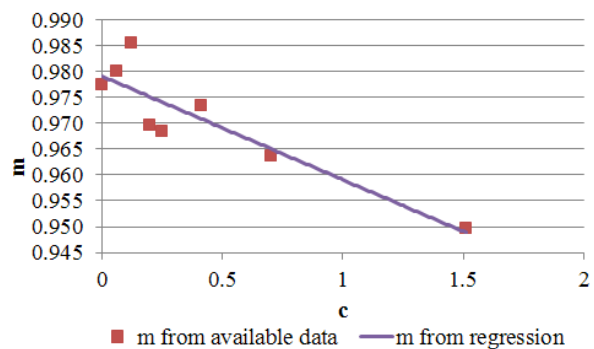


Fig. 6. Regression of the m coefficient on the concentration c . Dots represent available data.

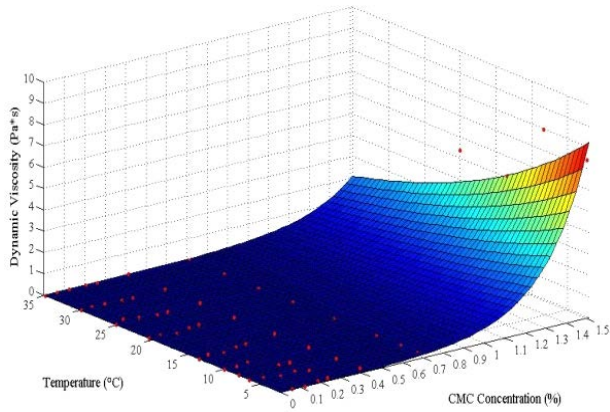


Fig. 7. The regressed spatial function $\mu_p(c,T)$, eq. (14).

The function $\mu_p(c,T)$ is represented by the surface drawn in Figure 7. Experimental data (red dots) are fitted quite well as the coefficient of determination is $R_2 = 0.9643$ and the RMSE is equal to 0.348.

5.2 From the prototype to the model

Passing from the prototype to the model is straight: solving eq. (9) for the viscosity μ_m yields:

$$\mu_m = 0,008290 \cdot e^{4,693c} \cdot (0,9790 - 0,01999 \cdot c)^T \cdot \frac{1}{\lambda^{3/2}} \tag{15}$$

The above function is not injective as different combinations (c,T) may give the same value of μ_m . In order to promptly setting the concentration to be used in laboratory, it is useful to define curves (c^*,T^*) at constant μ_m^* , see red lines in Figures 8 and 9. The equation of such curves is next given:

$$T^* = \frac{\ln \mu_m^* - \ln \alpha - \beta \cdot c^*}{\ln(\chi + \delta \cdot c^*)} \tag{16}$$

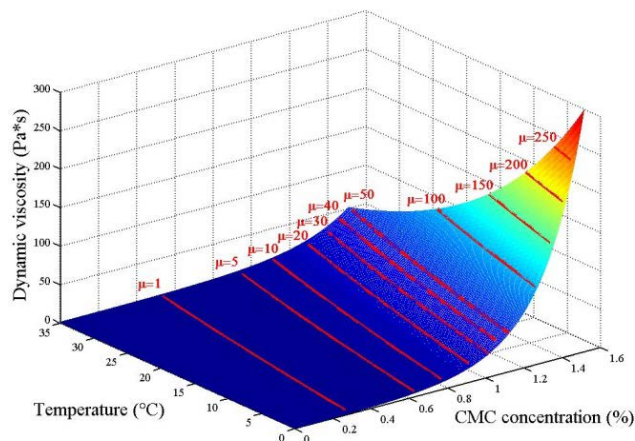


Fig. 8. The spatial function $\mu_m(c,T)$, eq. (15). Red lines define constant values as determined by eq. (17).

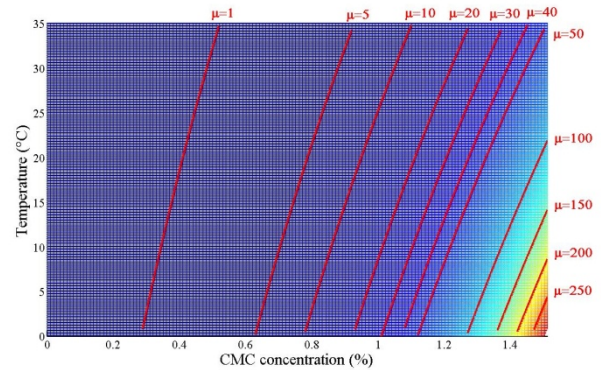


Fig. 9. Plain view of the function $\mu_m(c,T)$, eq. (15). The concentration of CMC can be derived by interpolation, knowing the operating temperature T and the viscosity μ_m of the real event.

that is, substituting constants $\alpha, \beta, \chi, \delta$ (see section 5.1):

$$T^* = \frac{\ln \mu_m^* + 4,792 - 4,693 \cdot c^*}{\ln(0,9790 - 0,01999 \cdot c^*)} \tag{17}$$

Conclusions

Sodium Carboxymethylcellulose (Na-CMC) can be used as viscosity modifier for simulating the interstitial fluid, filling pores in laboratory debris flows. CMC-water solutions can be considered as Newtonian fluids for their slightly pseudo-plastic behaviour under low rates of deformations. The related transparency make them particularly suitable in experimentation as the kinematics of a mass movement process can be easily described at walls using PIV techniques.

In order to model interstitial fluids of real debris flows events or simply mudflows, we established a simple double similitude model of Reynolds and Froude, obtaining a relationship between dynamic viscosities in the model and in the assumed prototype (eq. 8). As an example, assuming a particular spatial scale λ , we then derived model viscosities μ_m for real mudflows events analyzed in [21].

Viscometric tests carried at different CMC concentrations c and temperatures T allowed to first define the viscosity function $\mu_p(c,T)$ in the assumed prototype by calibrating coefficients appearing in

eq. (13). Applying the proposed similitude model we then derived the viscosity function $\mu_m(c,T)$ in the model (eq. 15) by simply scaling eq. (13) and finally the concentration c to be used in laboratory. Curves (c^*,T^*) at constant μ_m^* can be readily derived as depicted in Figure 9.

References

- [1] J. E. Costa, 1984, Physical geomorphology of debris flows, In: J. E. Costa and P. J. Fleischer (eds), *Developments and Applications of Geomorphology*, Springer, Berlin, Germany, pp. 268–317.
- [2] T. Takahashi, 1991, Debris Flow, IAHR Monograph Series, Balkema, Rotterdam, The Netherlands.
- [3] C. Hong-Kai, T. Hong-Mei, 2007, Essential Principle of debris flow dynamics. *Proceedings of the 4th WSEAS International Conference on Fluid Mechanics*, Gold Coast, Queensland, Australia, January 17-19, 2007, pp. 147-151.
- [4] D. L. George & R. M. Iverson, 2011, A Two-phase debris flow model that includes coupled evolution of volume fractions, granular dilatancy, and pore-fluid pressure. *Italian Journal of Engineering Geology and Environment*, pp. 415-424.
- [5] A. Armanini, L. Fraccarollo, G. Rosatti, 2009, Two-dimensional simulation of debris flows in erodible channels. *Computers & Geosciences*, 35, pp. 993–1006.
- [6] T. Takahashi, 1987. High velocity flow in steep erodible channels: *Proc. IAHR Congress, Lausanne*, pp. 42-53.
- [7] G. Viccione, S. Ferlisi, E. Marra, 2015, A numerical investigation of the interaction between debris flows and defense barriers, in: A. Bulucea, G. Viccione, C. Guarnaccia (Editors), *Advances in Environmental and Geological Science and Engineering, Proceedings of the 8th International Conference on Environmental and Geological Science and Engineering (EG '15)*, Salerno, Italy, June 27-29, Vol. 38, pp. 332 -342.
- [8] D. Laigle, A two-dimensional model for the study of debris-flow spreading on a torrent debris fan, 1997, in: C.L. Chen (Editor), *Debris-Flow Hazards Mitigation: Mechanics, Prediction and Assessment*, ASCE, pp. 123-132.
- [9] P. Coussot, D. Laigle, M. Arattano, A. Deganutti, L. Marchi, 1998, Direct determination of rheological characteristics of debris flow, *J. Hydraul. Eng.* 124(8), pp. 865-868.
- [10] J. Hübl, H. Steinwendtner, 2000, Estimation of rheological properties of viscous debris flows using a belt conveyor, *Phys. Chem. Earth, Part B* 25(9), pp. 751-755.
- [11] Iverson, R.M., 2003, The debris-flow rheology myth. In Rickenmann D. & Chen C.-L., EDS., *Debris flow Hazard Mitigation: Mechanics, Prediction and Assessment*, Millpress, Rotterdam, 1, pp. 303-314
- [12] M. Genovese, G. Viccione, F. Rossi, D. Guida, T.L.L. Lenza, 2014, Using the Sodium Carboxymethylcellulose (CMC) as viscosity modifier to model the interstitial fluid in laboratory debris flows, in: G. Viccione, C. Guarnaccia (Editors), *Latest Trends in Engineering Mechanics, Structures, Engineering Geology, Proceedings of the 7th International Conference on Engineering Mechanics, Structures, Engineering Geology (EMESEG '14)* Salerno, Italy, June 3-5, 2014, 26, pp. 179 -186.
- [13] G. Viccione, M. Genovese, F. Rossi, D. Guida, T.L.L. Lenza, 2015, Experimental measuring of bed shear stress in free surface flows, in: Recent Researches in Mechanical and Transportation Systems, *Proceedings of the 6th International Conference on Theoretical and Applied Mechanics (TAM '15)*, Salerno, Italy, June 27-29, 2015, 47, pp. 48-53.
- [14] P. Coussot, F. Bertrand & B. Herzhaft, 2004, Rheological Behavior of Drilling Muds, Characterization Using MRI Visualization. *Oil & Gas Science and Technology*, 59(1), pp. 23-29.
- [15] G. Seminara, 1993, Debris Flows: Meccanica, Controllo e Previsione, *Pubblicazioni del CNR-GNDCI*, 1429.
- [16] R. A. Bagnold, 1954. Experiments on a gravity-free dispersion of large solid spheres in a Newtonian Fluid under shear. *Proc. Roy. Soc. London, Ser. A*, 225, pp. 49-63.
- [17] R.M. Iverson, 1997, The physics of debris flows, *Rev. Geophys.*, 35, pp. 245–296.
- [18] D. Rickenmann, 1999, Empirical relationships for debris flows, *Natural Hazards*, 19, pp. 47-77.
- [19] A. Armanini, 1991. Physical Modelling of Debris-Flow, Atti di: *International Symposium on Debris Flow and Flood Disaster*, Emeishan City, China.
- [20] Hercules Inc., 1999, Aqualon®- Sodium carboxymethylcellulose. Physical and Chemical properties.
- [21] J. S. O'Brien and P. Y. Julien, 1988. Laboratory Analysis of mudflow properties. *J. Hydraul. Eng.*, 114, pp. 877-887.
- [22] G. Viccione, V. Bovolin, 2011, Simulating Triggering and Evolution of Debris-Flows with Smoothed Particle Hydrodynamics (SPH). *Italian Journal of Engineering Geology and Environment*, pp. 523-532.
- [23] L. Fraccarollo, M. N. Papa, 2000, Numerical simulation of real debris-flow events, *Phys. Chem. Earth, Part B*, 25(9), pp. 757-763.
- [24] J. Imran, G. Parker, J. Locat, H. Lee, 2001, 1D Numerical model of muddy subaqueous and subaerial debris flows, *J. Hydraul. Eng.*, 127(11), pp. 959-967.
- [25] B. Zanuttigh, A. Lamberti, 2004, Numerical modelling of debris surges based on shallow-

- water and homogeneous material approximations, *J. Hydraul. Res.*, 42(4), pp. 376-389.
- [26] P. Brufau, P. Garcia-Navarro, P. Ghilardi, L. Natale, F. Savi, 2000, 1D Mathematical modelling of debris flow, *J. Hydraul. Res.*, 38(6), pp. 435-446.
- [27] C.L. Shieh, C.D. Jan, Y.F. Tsai, 1996, A numerical simulation of debris flow and its applications, *Nat. Hazards*, 13, pp. 39-54.
- [28] R.M. Iverson, R.G. LaHusen 1993, Friction in debris flows: Inferences from Large-scale Flume Experiments, *Pr. Of the 1993 Hydraulic engineering conference*, San Francisco, California, pp. 1604–1609.
- [29] R.M. Iverson, 2003. The debris-flow rheology myth. In *Rickenmann D. & Chen C.-L.,EDS., Debris-flow Hazard Mitigation: Mechanics, Prediction and Assessment*, 1, pp. 303-314.
- [30] J. J. Major, T. C. Pierson, 1992, Debris flow rheology: experimental analysis of fine-grained slurries, *Wat. Resour. Res.* 28(3), pp. 841–857.
- [31] A.M. Johnson, 1970, Physical processes in geology: *Freeman, Cooper, San Francisco*, pp. 1-577.
- [32] T. Takahashi, 1978. Mechanical characteristics of debris flow: *J. Hydraul. Eng., ASCE*, 104, pp. 1153-1169.
- [33] T. Takahashi, 1993. Fluid mechanical modelling of viscous debris flow: *Proc. Pierre Beghin Intern. Workshop on Rapid Gravitational Mass Movements*, Open file.
- [34] P. Filip, J. Avid, 2013, Non-monotonous behaviour of shear viscosity – empirical modeling, *Recent Advances in Automatic Control, Modelling and Simulation*. ISBN: 978-1-61804-177-7, pp.41-44.
- [35] L. Sarno, M. N. Papa, R. Martino, 2011, Dam-break flows of dry granular materials on gentle slopes, *Italian Journal of Engineering Geology and Environment*, pp. 503-512.
- [36] B. W. McArdell, P. Bartelt, J. Kowalski, 2007, Field observations of basal forces and fluid pore pressure in a debris flow. *Geophysical Research Letters*, 34, pp. 303-326.